



## Aroma formation in retentostat co-cultures of *Lactococcus lactis* and *Leuconostoc mesenteroides*

Oscar van Mastrigt, Reinier A. Egas, Tjakko Abee, Eddy J. Smid\*

Food Microbiology, Wageningen University & Research, the Netherlands

### ARTICLE INFO

#### Keywords:

Mixed culture  
Cheese  
Fermentation  
Near-zero growth rate  
Interaction

### ABSTRACT

*Lactococcus lactis* subsp. *lactis* biovar diacetylactis and *Leuconostoc mesenteroides* are considered to be the main aroma producers in Dutch-type cheeses. Both species of lactic acid bacteria were grown in retentostat mono- and co-cultures to investigate their interaction at near-zero growth rates and to determine if co-cultivation enhances the aroma complexity compared to single species performance. During retentostat mono-cultures, the growth rates of both species decreased to less than  $0.001 \text{ h}^{-1}$  and a large fraction of the cells became viable but not culturable. Compared to *Lc. mesenteroides*, *L. lactis* reached a 3.4-fold higher biomass concentration caused by i) a higher ATP yield on substrate, ii) a higher biomass yield on ATP and iii) a lower maintenance requirement ( $m_{\text{ATP}}$ ). Dynamic models estimated that the  $m_{\text{ATP}}$  of both species decreased approximately 7-fold at near-zero growth rates compared to high growth rates. Extension of these models by assuming equal substrate distribution resulted in excellent prediction of the biomass accumulation in retentostat co-cultures with *L. lactis* dominating (100:1) as observed in ripened cheese. Despite its low abundance ( $\sim 1\%$ ), *Lc. mesenteroides* contributed to aroma production in co-cultures as indicated by the presence of all 5 specific *Lc. mesenteroides* compounds. This study provides insights in the production of cheese aroma compounds outside the cheese matrix by co-cultures of *L. lactis* and *Lc. mesenteroides*, which could be used as food supplements in dairy or non-dairy products.

### 1. Introduction

Mesophilic mixed DL-type starter cultures used for the production of Dutch-type cheeses consist of the homofermentative *Lactococcus lactis* subsp. *cremoris*, *Lactococcus lactis* subsp. *lactis*, *Lactococcus lactis* subsp. *lactis* biovar diacetylactis and the heterofermentative *Leuconostoc* spp. (Frantzen et al., 2017). *L. lactis* subsp. *cremoris* and *L. lactis* subsp. *lactis* are considered to be the main acid producers that dominate in the early stages of cheese making and quickly decline during cheese ripening (Erkus et al., 2013). In contrast, *L. lactis* subsp. *lactis* biovar diacetylactis and *Leuconostoc* spp. become dominant during cheese ripening due to better survival and are the main aroma and texture producers. The aroma producers generally account for 1–10% of the starter culture population (Cogan and Jordan, 1994; Erkus et al., 2013). Both species are able to metabolise citrate and produce the important flavours diacetyl and acetoin as well as  $\text{CO}_2$ , which is important for eye formation (Hugenholz, 1993). Other important aroma compounds in cheese result from the metabolism of fatty acids and amino acids of which aromatic, sulphur-containing and branched-chain amino acids are considered to be most important (Yvon and Rijnen, 2001).

Recently, it was demonstrated that aroma formation by *L. lactis*

subsp. *lactis* biovar diacetylactis was greatly affected by slow growth of the bacteria using retentostat cultivation, thereby better resembling aroma formation during cheese ripening (van Mastrigt et al., 2018b). Retentostat cultivation is a modification of chemostat cultivation in which a filter is connected to the effluent line thereby recycling the biomass to the bioreactor (Boender et al., 2009). This leads to accumulation of the biomass in time and a severe reduction in growth rate that approaches zero. Growth rates below  $0.001 \text{ h}^{-1}$  were obtained with the dairy *L. lactis* biovar diacetylactis FM03-V1 (van Mastrigt et al., 2018a). In addition to changes in aroma formation, the number of viable but non-culturable cells increased and the maintenance requirements decreased most likely due to a decrease in the energy spent on protein turnover (van Mastrigt et al., 2018a).

While studying aroma formation by lactic acid bacteria using retentostat cultivation, it has to be taken into account that starter cultures often consist of multiple strains and species. Metabolic complementation of strains could result in new compounds that cannot be produced by the single strains, thereby increasing the aroma complexity. Such complementation has been suggested for *L. lactis* and *Lc. mesenteroides* for the conversion of glutamate into succinate (Erkus et al., 2013).

To study such interactions under relevant conditions for cheese

\* Corresponding author. Food Microbiology, Wageningen University & Research, P.O. Box 17, 6700AA, Wageningen, the Netherlands.  
E-mail address: [eddy.smid@wur.nl](mailto:eddy.smid@wur.nl) (E.J. Smid).

ripening, i.e. slow growth, *L. lactis* biovar diacetylactis FM03-V1 and *Lc. mesenteroides* FM06 were grown in retentostat mono- and co-cultures and the production of aroma compounds was compared. Moreover, dynamic models were developed to describe growth in retentostat mono-cultures and these models were used to predict growth of both species in retentostat co-cultures to identify growth stimulating or inhibiting interactions between the species. Finally, this study provides insights in the production of cheese aroma compounds outside the cheese matrix by co-cultures of *L. lactis* and *Lc. mesenteroides*, which could be applied as food supplements in dairy or non-dairy products.

## 2. Material and methods

### 2.1. Strains and media

In this study *Lactococcus lactis* subsp. *lactis* biovar diacetylactis FM03-V1 and *Leuconostoc mesenteroides* FM06 were used, which were both isolated from 10-week-old Samsø cheese (van Mastrigt et al., 2017). For chemostat and retentostat cultivation, the bacteria were streaked from a  $-80^{\circ}\text{C}$  stock onto M17 agar plates supplemented with 0.5% (w/v) lactose (LM17) and MRS plates respectively, and incubated for 2 days at  $30^{\circ}\text{C}$ . A single colony was transferred to 10 ml lactose-containing chemically defined medium (van Mastrigt et al., 2018c) and grown overnight at  $30^{\circ}\text{C}$ . The bioreactors were inoculated with the overnight culture at a 1% (v/v) inoculated level. The lactose-limited chemically defined medium used for the pre-cultures and the chemostat and retentostat cultivations contained 0.5% (w/w) lactose, 10 mM  $(\text{NH}_4)_3\text{citrate}$  and 1% (w/w) Bacto-tryptone (van Mastrigt et al., 2018c) and was prepared in 20 L batches.

### 2.2. Retentostat cultivation

Retentostat cultivations were performed in bioreactors with a working volume of 1 L (Infors HT, Switzerland) as previously described (van Mastrigt et al., 2018a). The stirring speed was set at 400 rpm, the temperature was maintained at  $30^{\circ}\text{C}$  and the pH was controlled at 5.5 by automatic addition of 5 M NaOH. Anaerobic conditions were maintained by flushing the headspace with nitrogen gas at 0.1 L/min. The optical density at 600 nm was continuously measured by an internal probe (TruCell 2, Finesse, USA). Retentostat cultivations were initiated by connecting a sterilisable polyethersulfone cross-flow filter (Spectrum laboratories, USA) to the effluent line after reaching a steady state in the chemostat cultivations at a dilution rate of  $0.025\text{ h}^{-1}$ . A steady state was considered to be achieved after a minimum of five volume changes at which the optical density remained constant. In case of co-cultivation, *L. lactis* and *Lc. mesenteroides* were pre-grown separately in 0.5 L chemostat cultures at a dilution rate of  $0.025\text{ h}^{-1}$  and, after achieving a steady state in both cultures, were transferred to a 1 L bioreactor equipped with a cross-flow filter to initiate the retentostat cultivation.

Bacteria were grown in retentostat mono- and co-cultures for 35 and 21 days, respectively. To determine the maximum biomass yield on ATP ( $Y_{X/\text{ATP}}^{\text{max}}$ ) and the maintenance coefficient ( $m_{\text{ATP}}$ ) of *L. lactis* FM03-V1 and *Lc. mesenteroides* FM06, the bacteria were grown in chemostat cultures at dilution rates between  $0.025$  and  $0.4\text{ h}^{-1}$ .

### 2.3. Biomass determination

To monitor the biomass accumulation in the chemostat and retentostat cultures, the cell dry weight concentration was measured as previously described (van Mastrigt et al., 2018c). Briefly, culture samples of 3–4 ml were taken directly from the bioreactor and passed through pre-weighted  $0.2\text{ }\mu\text{m}$  membrane filters (Pall Corporation, USA) by a vacuum filtration unit. The filters were dried at  $80^{\circ}\text{C}$  for at least 2 days and weighted again to determine the dry weight of cell biomass.

### 2.4. Cell counts

To determine the total number of cells in the continuous cultures, samples were diluted 1000 times with physiological salt solution (PPS; Tritium Microbiologie, The Netherlands) and  $25\text{ }\mu\text{l}$  of this diluted suspension was added to a Bürker-Türk counting chamber (CellVision technologies, Netherlands). Cells were counted at 1000 times ( $10 \times 100$ ) magnification using a phase contrast microscope (Olympus, Japan).

### 2.5. Plate counts

To quantify the number of colony forming units (CFU), appropriate dilutions of the cultures in PPS were plated on agar plates and the number of CFUs were counted after incubation for 3 days at  $30^{\circ}\text{C}$ . For mono-cultures, MRS and LM17 plates were used to quantify *Lc. mesenteroides* and *L. lactis*, respectively. For co-cultures, MRS supplemented with 30 mg/L vancomycin, LM17 and MRS plates were used to quantify *Lc. mesenteroides*, *L. lactis* and both bacteria, respectively.

### 2.6. Cell viability

The viability of the cultures was determined by LIVE/DEAD BacLight Bacterial Viability kit (Molecular Probes Europe, Netherlands). Bacteria were strained with  $3.34\text{ }\mu\text{M}$  green fluorescent SYTO 9 and  $20\text{ }\mu\text{M}$  red fluorescent propidium iodide for 10 min at room temperature in the dark. Green and red fluorescent cells were visualised using a fluorescence microscope with an excitation light source (Excelitas, USA) at 630 or 1000 times magnification. Pictures were taken with a camera attached to the microscope and the number of green and red cells was counted manually.

### 2.7. Determination of viable *L. lactis* and *Lc. mesenteroides* in co-cultures

The ratio of viable cells of *L. lactis* and *Lc. mesenteroides* in co-cultures was determined in three steps: i) propidium monoazide (PMA) treatment, ii) DNA extraction and iii) quantitative PCR (qPCR) analysis. One ml culture with an optical density at 600 nm of 0.1 was centrifuged ( $17000 \times g$  for 5 min) and washed with  $500\text{ }\mu\text{l}$  phosphate buffered saline (PBS) and resuspended in 1 ml PBS. Subsequently,  $2.5\text{ }\mu\text{l}$  20 mM PMA was added and the cell suspension was incubated for 5 min in the dark at room temperature with mixing every minute. The samples were exposed to light for 5 min with a PMA-Lite™ led photolysis device (Biotium, USA) to activate the PMA. DNA was extracted using the DNeasy Blood and Tissue kit (Qiagen, Germany) according to the manufacturer's instructions with some modifications: 50 Units mutanolysin were added to the lysis buffer and DNA was eluted with three times  $50\text{ }\mu\text{l}$  AE buffer. Purified DNA was stored at  $-20^{\circ}\text{C}$  until analysis with qPCR. DNA extraction efficiencies of *L. lactis* and *Lc. mesenteroides* were compared by extraction of DNA in triplicate from chemostat mono-cultures at a dilution rate of  $0.025\text{ h}^{-1}$  according to the above protocol. This showed that extraction efficiencies of both species were not significantly different (*t*-test assuming equal variances, two-sided, degrees of freedom = 4, *t* value =  $-1.26$ , *P* value = 0.27). DNA of *L. lactis* and *Lc. mesenteroides* were quantified with qPCR (Bio-Rad Thermal cycler CFX96-Real-Time system) targeting the single-copy gene *glyA* and using TaqMan probes. Sequences of the used primers and probes are given in Table 1. The PCRs took place in  $20\text{ }\mu\text{l}$  reaction mixtures containing 0.2 mM dNTPs,  $0.5\text{ }\mu\text{M}$  forward primer,  $0.5\text{ }\mu\text{M}$  reverse primer,  $0.31\text{ }\mu\text{M}$  TaqMan probe,  $2\text{ }\mu\text{l}$  10x DreamTaq buffer with  $\text{MgCl}_2$  (Thermo Scientific, USA), 0.8 U DreamTaq polymerase and  $2\text{ }\mu\text{l}$  purified DNA. PCR amplification was initiated with 5 min at  $95^{\circ}\text{C}$  followed by 39 cycles of 10 s at  $95^{\circ}\text{C}$  and 20 s at  $59^{\circ}\text{C}$ . Fluorescence was measured at the end of each cycle. A threshold of 400 relative fluorescence unit (RFU) was used to determine the threshold cycle ( $C_t$ ). The efficiency of the PCRs of both species was not significantly different

**Table 1**  
Primer and TaqMan probes used to quantify viable *L. lactis* and *Lc. mesenteroides* in retentostat co-cultures with qPCR.

	Sequences (5'→ 3')		Amplicon (bp)
<i>L. lactis</i>	Fw	CAAAAGCAGTTATGGCAGCA	100
	Rv	ACATCAACCGCTTCTGTTC	
	Probe	[6FAM]ACGTTTCCCAGGATAACCTTCGGC[BHQ1]	
<i>Lc. mesenteroides</i>	Fw	AAGTTTCGTGCGATTGCTG	105
	Rv	ATGCCTACTGGATTGGGATG	
	Probe	[6FAM]CAAGTCCGGCAATATGCGCCA[BHQ1]	

from 2 (mean  $\pm$  standard error was  $2.04 \pm 0.10$  and  $2.03 \pm 0.03$  for *L. lactis* and *Lc. mesenteroides*, respectively). Therefore, an efficiency of 2 was used to calculate the ratio of *L. lactis*:*Lc. mesenteroides* in the co-cultures using equation (1):

$$L. lactis: Lc. mesenteroides = 2^{C_{tLM} - C_{tLL}} \quad (1)$$

To calculate the viability of *Lc. mesenteroides* during the co-cultures, qPCR was also performed using DNA without a PMA treatment, which showed that the viability was at least 33% throughout the co-cultures.

## 2.8. Analysis of extracellular metabolites

Lactose, citrate, lactate, acetate, ethanol, formate, pyruvate and acetoin were quantified every 3–4 days in retentostat cultures by High Performance Liquid Chromatography (HPLC) as previously described (van Mastrigt et al., 2018c). Briefly, we used an Ultimate 3000 instrument (Dionex, Germany) equipped with an Aminex HPX-87H column (Bio-Rad, USA) with pre-column at 40 °C and 5 mM H<sub>2</sub>SO<sub>4</sub> was used as mobile phase at 0.6 ml/min. Compounds were detected with a Shodex RI-101 refractive index detector (Showa DendoKK, Japan).

## 2.9. Volatile organic compounds analysis

Volatile organic compounds (VOCs) were analysed every 3–4 days in retentostat cultures by headspace solid phase microextraction gas chromatography mass spectrometry (HS SPME GC-MS) as previously described (van Mastrigt et al., 2018a). 100  $\mu$ l sample was incubated for 10 min at 60 °C and VOCs were extracted for 20 min at 60 °C using a SPME fiber (85 mm CAR/PDMS, Supelco, USA). Compounds were desorbed for 10 min on a Stabilwax<sup>®</sup>-DA-Crossband<sup>®</sup>-Carbowax<sup>®</sup>-polyethylene-glycol column (30 m length, 0.25 mm ID, 0.5  $\mu$ m df). PTV Splitless mode was used at 250 °C for 5 min. Helium was used as carrier gas at a constant flow of 1.5 ml/min. The temperature of the GC oven was initially 40 °C and after 2 min the temperature was raised to 240 °C at a rate of 10 °C/min and kept at 240 °C for 5 min. Mass spectral data was collected over a range of m/z 33–250 in full scan mode with 3.0030 scans/second. Aroma profiles were analysed using Chromeleon 4.2 software. Peaks were integrated using the ICIS algorithm and the mass spectral profiles were matched with the NIST main library for identification. One peak was used for quantification (in general the highest m/z peak per compound) and 1 or 2 peaks were used for confirmation. Analysis of uninoculated medium revealed compounds that were related to the medium (e.g. 1-butanol). These compounds were excluded from all analyses as well as their reaction products (e.g. esters of 1-butanol).

## 2.10. Principal component analysis

Principal component analysis (PCA) of the aroma profiles in mono- and co-cultures were performed in R (version 3.1.3) using scaled peak areas (mean peak area of every compound is 0 and standard deviation is 1).

## 2.11. Mathematical modelling of biomass accumulation

### 2.11.1. Mono-cultures

Biomass accumulation in the retentostat mono-cultures were modelled according to van Mastrigt et al. (van Mastrigt et al., 2018a) using equation (2).

$$C_X(t) = \left( C_{X,0} - \frac{D \cdot (C_{S,in} - C_S) \cdot Y_{ATP/S}}{m_{ATP}} \right) \cdot e^{-m_{ATP} \cdot Y_{X/ATP}^{max} \cdot t} + \frac{D \cdot (C_{S,in} - C_S) \cdot Y_{ATP/S}}{m_{ATP}} \quad (2)$$

in which  $C_X$  is the biomass concentration (gDW/kg),  $C_{X,0}$  is the initial biomass concentration (gDW/kg),  $D$  is the dilution rate ( $h^{-1}$ ),  $C_{S,in}$  is the substrate concentration in the medium (14.6 mmol/kg lactose and 10 mmol/kg citrate),  $C_S$  is the substrate concentration in the effluent,  $Y_{ATP/S}$  is the ATP yield on substrate (mol ATP/CmolS),  $m_{ATP}$  is the maintenance coefficient (mol ATP-gDW<sup>-1</sup>·h<sup>-1</sup>),  $Y_{X/ATP}^{max}$  is the maximum biomass yield on ATP (gDW/mol ATP) and  $t$  is the time (h). The  $Y_{ATP/S}$  was calculated based on the measured metabolite production rates using equations (3) and (4) for *L. lactis* and *Lc. mesenteroides*, respectively.

$$R_{ATP/S,LL} = \frac{R_{lactate} + R_{ethanol} + R_{pyruvate} + 2 \cdot R_{acetoin} + 2 \cdot R_{acetate} + 2 \cdot R_{citrate}}{-(12 \cdot R_{lactose} + 6 \cdot R_{citrate})} \quad (3)$$

$$R_{ATP/S,LM} = \frac{0.5 \cdot R_{lactate} + 0.5 \cdot R_{ethanol} + 0.5 \cdot R_{pyruvate} + 1.5 \cdot R_{acetate} + R_{citrate}}{-(12 \cdot R_{lactose} + 6 \cdot R_{citrate})} \quad (4)$$

In these equations  $R_i$  is the production rate (mol/h) of compound  $i$  and it was assumed that uptake of 1 mol citrate and its conversion to pyruvate generated 1 mol ATP for both bacteria.

The  $Y_{X/ATP}^{max}$  was estimated in chemostat cultures with a dilution rate between 0.025 and 0.4  $h^{-1}$ . The  $m_{ATP}$  was assumed to be linearly dependent on the biomass specific ATP production rate ( $q_{ATP}$ ) with a maximum  $m_{ATP}^{max}$  (Eq. (4)).

$$m_{ATP} = a + b \cdot q_{ATP} \text{ with } m_{atp} \leq m_{ATP}^{max} \quad (5)$$

Input data for the modelling were online optical density measurements, which were converted to cell dry weight concentrations using a second-order polynomial relation. The variable parameters ( $a$ ,  $b$  and  $m_{ATP}^{max}$  in equation (4)) were optimised by minimising the sum of squared errors between the model and the data in 10 min intervals using the solver add-in of Microsoft Excel.

### 2.11.2. Co-cultures

The optimised variable parameters of the mono-cultures were used in a co-culture model to predict the biomass accumulation of *L. lactis* and *Lc. mesenteroides* in the co-cultures. The co-culture model followed the mono-culture model with the addition that we assumed i) equal uptake kinetics of both species for lactose and citrate, in other words substrate consumption was divided over both species based on the biomass concentration and ii) no lysis of the species even when  $q_{ATP} < m_{ATP}$ .

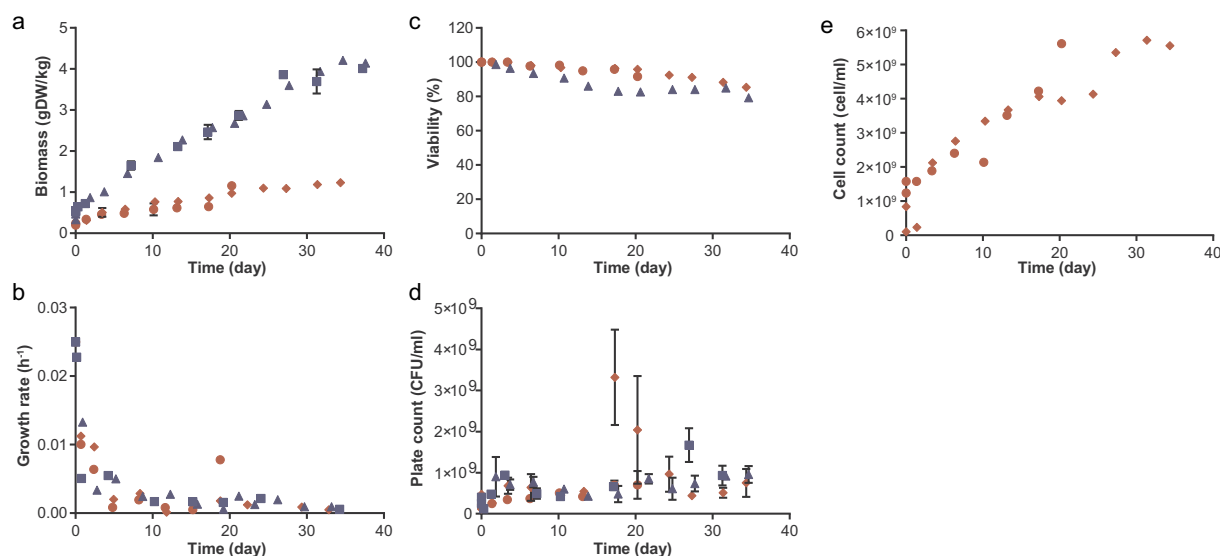


**Fig. 1.** Growth of *L. lactis* FM03-V1 (blue) and *Lc. mesenteroides* FM06 (red) in retentostat mono-cultures. Squares, triangles, diamonds and circles represent four independent retentostat cultures. At time 0 a chemostat culture in steady state was switched to retentostat mode by insertion of a filter in the effluent. **a:** Measured biomass concentrations. Data points represent the mean ± standard deviation of duplicate samples. **b:** Calculated growth rates based on the biomass concentrations. **c:** Viability determined using SYTO 9 and propidium iodide as fluorescent markers and fluorescent microscopy for visualisation. **d:** Plates counts of *L. lactis* and *Lc. mesenteroides* on LM17 and MRS, respectively. Data points represent the mean ± standard deviation. **e:** Microscopic cell counts determined using a counting chamber. (For interpretation of the references to colour in this figure legend, the reader is referred to the Web version of this article.)

### 3. Results

#### 3.1. Biomass accumulation in retentostat mono-cultures

*Lactococcus lactis* FM03-V1 and *Leuconostoc mesenteroides* FM06 were grown anaerobically in four independent retentostat mono-cultures on a chemically defined medium containing both lactose and citrate. The biomass concentration was measured every 3–4 days and the growth rates were estimated. Moreover, we quantified the number of colony forming units by plating on LM17 or MRS and the culture viability by live/dead staining with SYTO 9 and propidium iodide. The retentostat cultures of *L. lactis* has previously been described (van Mastrigt et al., 2018a).

For *L. lactis* and *Lc. mesenteroides* the biomass concentration increased to 4.2 and 1.2 gDW/kg, respectively, which corresponded to an 8 and 6-fold increase (Fig. 1a). The higher biomass concentration of *L. lactis* indicates a lower maintenance requirement, i.e. less substrate required to maintain cells and/or a higher biomass yield on substrate. The growth rate of both species gradually decreased to less than 0.001 h<sup>-1</sup>, corresponding to doubling times of more than a month (Fig. 1b). The viability remained above 80% throughout all cultivations (Fig. 1c). Despite the observed increases in biomass, the plate counts hardly increased during the cultivations (Fig. 1d) indicating that a large fraction of the cells became viable but not culturable (VBNC). This was confirmed for *Lc. mesenteroides* by microscopic cell counting (Fig. 1e), which showed a 6-fold increase similar to the observed increase in biomass concentration. This indicates that both species had very similar physiological responses towards near-zero growth rates.

#### 3.2. Central metabolism

The higher biomass concentration of *L. lactis* could be explained by the different metabolic pathways for lactose utilisation of both species. The homofermentative *L. lactis* uses the Embden-Meyerhof-Parnas (EMP) pathway producing 4 to 6 mol ATP per mol lactose when it produces lactate (homolactic fermentation) or formate, acetate and ethanol (mixed-acid fermentation), respectively. The heterofermentative *Lc. mesenteroides* uses the phosphoketolase pathway

producing only 2 mol ATP per mol lactose and equimolar amounts of lactate and ethanol. By using the co-substrate citrate as alternative electron acceptor (Schmitt et al., 1990), 1 extra ATP can be produced per mol citrate by *Lc. mesenteroides* via acetate kinase. The main substrates (lactose and citrate) and products (lactate, ethanol, acetate, formate, acetoin, pyruvate) were quantified with HPLC and the amount of ATP that they theoretically gained from lactose and citrate metabolism was calculated with equations (3) and (4) (Fig. 2). *L. lactis* mainly produced lactate, acetate, ethanol and formate via a combination of homolactic and mixed-acid fermentation (ratio of approximately 60:40), which resulted in approximately 0.33 mol ATP per Cmol substrate (lactose and citrate). *Lc. mesenteroides* produced mainly lactate, ethanol and acetate resulting in a ATP yield of 0.18 mol ATP per Cmol substrate (lactose and citrate). This confirmed our hypothesis that *L. lactis* metabolised the lactose and citrate more efficiently resulting in higher biomass concentrations in retentostat cultures. Interestingly, acetate production by *Lc. mesenteroides* via acetate kinase was very limited (on average 0.04 mmol/h) despite use of citrate. Possibly, acetate kinase was not very active due to the anaerobic conditions.

#### 3.3. Modelling of retentostat mono-cultures

Biomass accumulation in retentostat cultures was modelled according to a model described by van Mastrigt et al. (van Mastrigt et al., 2018a), assuming i) a constant maximum biomass yield on ATP ( $Y_{X/ATP}^{max}$ ) and ii) a maintenance coefficient ( $m_{ATP}$ ) that was linearly dependent on the biomass specific ATP production rate ( $q_{ATP}$ ). The  $Y_{X/ATP}^{max}$  and  $m_{ATP}$  of *L. lactis* and *Lc. mesenteroides* were determined in chemostat cultures at dilution rates between 0.025 and 0.4 h<sup>-1</sup> (Fig. 3).

*L. lactis* had a higher  $Y_{X/ATP}^{max}$  than *Lc. mesenteroides* (mean ± SE; 15.94 ± 0.42 and 9.52 ± 0.73 gDW/mol ATP) and a lower  $m_{ATP}$  (mean ± SE; 2.43 ± 0.35 and 5.32 ± 0.93 mmol ATP·gDW<sup>-1</sup>·h<sup>-1</sup>) contributing to the higher biomass concentrations in the retentostat cultures. The determined maximum biomass yields on ATP were included in the model and the biomass accumulation was fitted with the model (as described in section 2.11.1 in the material and methods). Good fits were obtained for retentostat cultures of both *L. lactis* and *Lc. mesenteroides* (root mean square error of 0.098, 0.028, 0.020 and

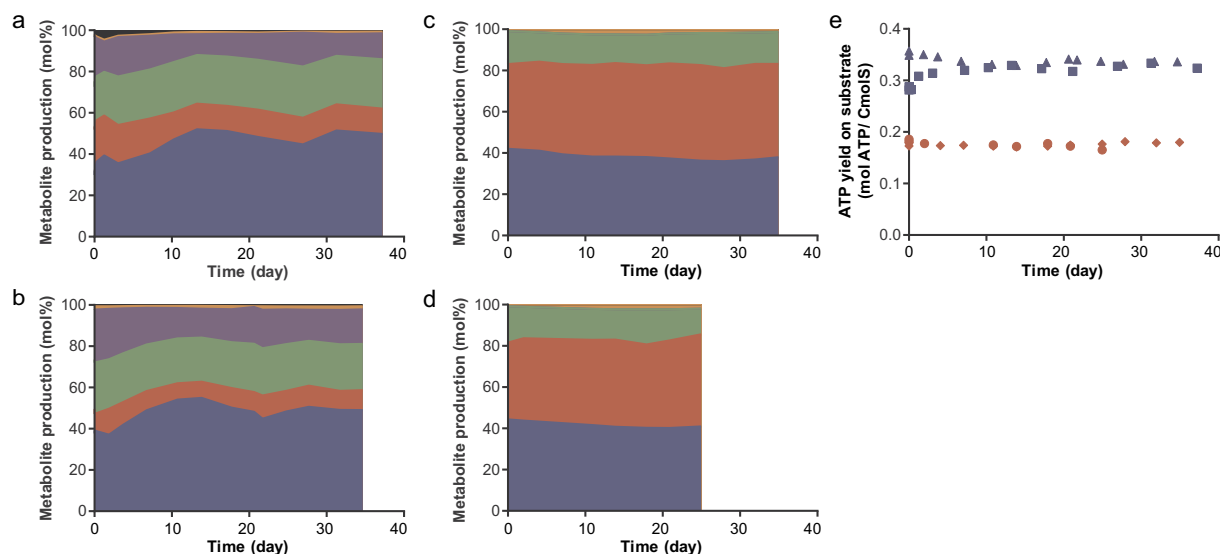


**Fig. 2.** Metabolite production of *L. lactis* (a and b) and *Lc. mesenteroides* (c and d) and the calculated ATP yield on substrate (e). At time 0 a chemostat culture in steady state was switched to retentostat mode by insertion of a filter in the effluent. Electron-balances, which were calculated using the degree of reduction of the main substrate and products, were always between 94 and 106%. Metabolite production was normalised to 100%. a, b, c, d: Blue, red, green, purple, orange and black represent lactate, ethanol, acetate, formate, pyruvate and acetoin, respectively. e: The ATP yield on substrate ( $Y_{ATP/S}$ ) (lactose and citrate) was calculated based on the metabolite production profiles and the known metabolism of *L. lactis* and *Lc. mesenteroides*. We assumed that 1 ATP was produced by uptake and conversion of citrate into pyruvate. (For interpretation of the references to colour in this figure legend, the reader is referred to the Web version of this article.)

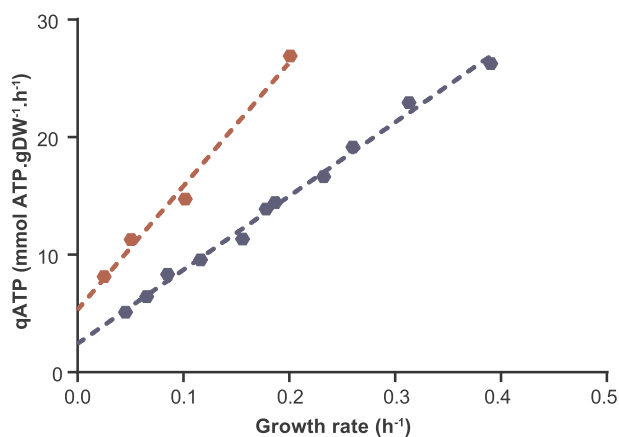


**Fig. 3.** Relation between the specific growth rate and the biomass specific ATP production rate (qATP) in chemostat cultures of *L. lactis* (blue) and *Lc. mesenteroides* (red). The dotted lines represent regression lines used to determine the maximum biomass yield on ATP ( $Y_{X/ATP}^{max}$ ) (1/slope) and the maintenance coefficient ( $m_{ATP}$ ) (intercept with y-axis). (For interpretation of the references to colour in this figure legend, the reader is referred to the Web version of this article.)

0.094 gDW/kg, respectively) (Fig. 4). The model predicted that the maintenance coefficient of *L. lactis* and *Lc. mesenteroides* decreased approximately 7-fold at near-zero growth rates to 0.36 and 0.79 mmol ATP·gDW<sup>-1</sup>·h<sup>-1</sup>, respectively (Suppl. Fig. S1).

### 3.4. Biomass accumulation on retentostat co-cultures

The models of the retentostat mono-cultures were combined to predict growth of *L. lactis* and *Lc. mesenteroides* in retentostat co-cultures. It was assumed that both species had similar substrate uptake kinetics, in other words that substrate was divided over both species depending on their biomass concentration. Moreover, it was assumed that cells did not lyse when the available substrate was less than their maintenance requirement. The model was compared with two independent retentostat co-cultures in which we determined i) the total

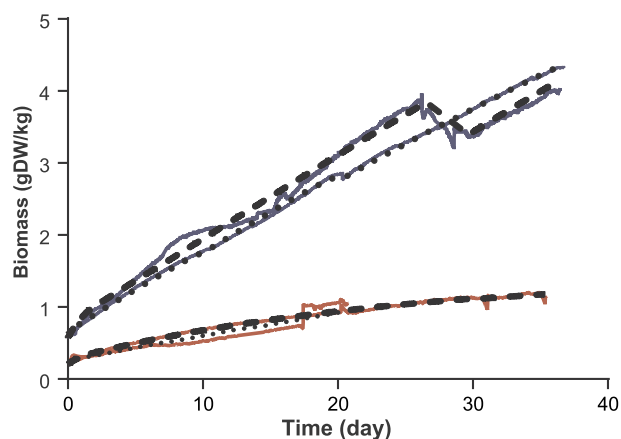


**Fig. 4.** Model predictions of the biomass in retentostat mono-cultures of *L. lactis* (blue) and *Lc. mesenteroides* (red). At time 0 a chemostat culture in steady state was switched to retentostat mode by insertion of a filter in the effluent. The solid lines represent the online optical density measurements that were converted to cell dry weights with a second-order polynomial function. The dashed and dotted lines represent the model predictions. (For interpretation of the references to colour in this figure legend, the reader is referred to the Web version of this article.)

cell dry weight and ii) the relative abundance of both species. The relative abundance was determined using selective plates: LM17 for *L. lactis* and MRS supplemented with vancomycin for *Lc. mesenteroides*. Because we found an increase in viable but non-culturable cells in retentostat mono-cultures of both *L. lactis* and *Lc. mesenteroides*, we also determined the relative abundance using qPCR with a propidium monoazide (PMA) treatment (Erkus et al., 2016) to specifically amplify DNA of viable cells. Relative abundances of selective plating and qPCR were very similar (Suppl. Fig. S2). Compared to *Lc. mesenteroides*, the relative abundance of *L. lactis* increased during the retentostat co-cultivations from a ratio of approximately 2.5:1 to 100:1. Based on the total cell dry weight and selective plate counts, dry weights of *L. lactis* cells and *Lc. mesenteroides* in the retentostat co-cultures were calculated and compared with our model prediction (Fig. 5). The model predicted

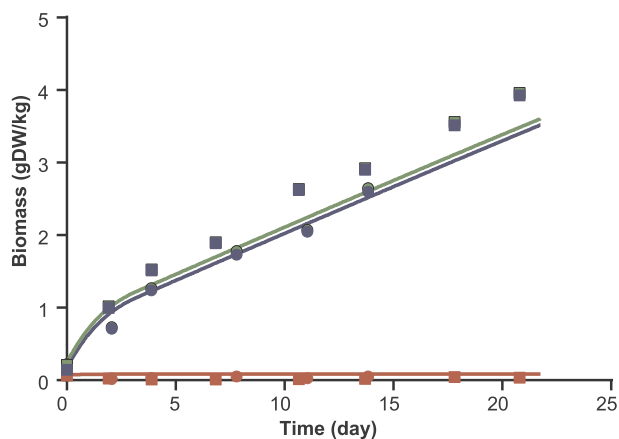


**Fig. 5.** Measured and predicted biomass accumulation of *L. lactis* (blue) and *Lc. mesenteroides* (red) in retentostat co-cultures. At time 0 chemostat cultures of *L. lactis* and *Lc. mesenteroides* were combined and switched to retentostat mode by insertion of a filter in the effluent. The total cell dry weight concentration (green symbols) was multiplied with the fraction of both species, determined by plates counts on selective plates (Suppl. Fig. S2), to obtain the estimated biomass concentration of *L. lactis* and *Lc. mesenteroides*. Squares and circles represent measurements of two independent co-cultures. The lines represent the model predictions as explained in section 2.11.2 of the material and methods. (For interpretation of the references to colour in this figure legend, the reader is referred to the Web version of this article.)

the biomass concentration of both species very well indicating that competition was mainly at the level of nutrient acquisition and no growth stimulation or additional inhibiting interactions were found.

### 3.5. Aroma formation in retentostat mono- and co-cultures

During the retentostat mono- and co-cultures, samples were taken to analyse the production of volatile organic compounds (VOCs) by headspace SPME GC-MS. In total 47 aroma compounds were considered produced after exclusion of medium-associated compounds (see section 2.9 in the material and methods). To get an overview of the differences between aroma production mono- and co-cultures of *L. lactis* and *Lc. mesenteroides*, we performed a principal component analysis (PCA) (Fig. 6).

Aroma profiles of mono-cultures of *L. lactis* and *Lc. mesenteroides* were clearly separated indicating bigger differences in aroma production between the species than between the cultivations with the same species. A trend in time was visible for the *L. lactis* mono-cultures indicating that aroma production changed at near-zero growth rates. Aroma profiles of the co-cultures were separated from both the mono-cultures of *L. lactis* and *Lc. mesenteroides* indicating that *Lc. mesenteroides* contributed to formation of aroma compounds despite its low abundance. Furthermore, the aroma profiles of the co-cultures showed a trend in time, which most likely was caused by the gradual increase in relative abundance of *L. lactis* in the co-cultures.

Comparison of the abundances of aroma compounds in mono-cultures revealed that 17 and 5 out of the 47 compounds were mainly produced at low growth rates by *L. lactis* and *Lc. mesenteroides*, respectively (at least 8-fold difference in maximum abundance between species) (Fig. 7). All aroma compounds specific for *L. lactis* except ethyl decanoate were found in the co-cultures, but the abundance of 7 aroma compounds specific for *L. lactis* severely decreased (> 8-fold difference in maximum abundance) compared to the mono-cultures (2,3-pentanedione, ethyl hexanoate, ethyl octanoate, 1-tetradecanol, 1-hexadecanol, 2,6-dimethylpyrazine and trimethylxazole) (Fig. 7 and Fig. 8). This indicates that either *Lc. mesenteroides* affected the production of these compounds by *L. lactis* or these compounds were consumed by *Lc. mesenteroides*. Because only 1% of the population in

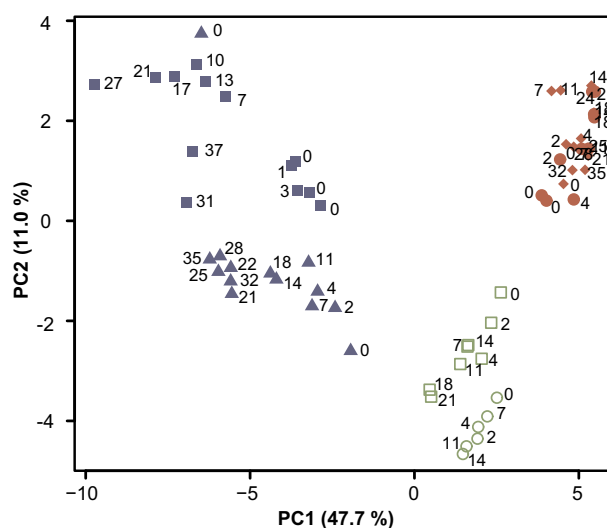


**Fig. 6.** Principal component analysis (PCA) of aroma profiles produced in retentostat mono-cultures of *L. lactis* (blue) and *Lc. mesenteroides* (red) and of co-cultures (green). Squares, triangles, diamonds and circles represent independent retentostat cultivations. The numbers near the symbols correspond to the time in the retentostat after inserting the filter in the effluent. The x and y-axis correspond to principal components 1 and 2, respectively, and the variance that they explained is given in parentheses. (For interpretation of the references to colour in this figure legend, the reader is referred to the Web version of this article.)

the co-cultures was *Lc. mesenteroides*, abundances of aroma compounds specific for *Lc. mesenteroides* were expected to be lower than in the mono-cultures. The maximum abundance of ethyl acetate, ethyl lactate and 2-propanol in the co-cultures was indeed only 10.4%, 0.3% and 0.7% of the maximum abundance in the *Lc. mesenteroides* mono-cultures. Surprisingly, 2 out of 5 compounds specific for *Lc. mesenteroides* (2-ethyl-1-hexanol and 1-decanol) were present in the co-cultures at similar levels as in the mono-cultures (Fig. 8). No additional unique compounds were produced in the co-cultures indicating that interaction between the species at the level of metabolic complementation and/or cross-feeding did not result in additional aroma compounds.

## 4. Discussion

*Lactococcus lactis* biovar diacetylactis and *Leuconostoc* spp. are considered to be the main aroma producers in mesophilic DL-type starter cultures to make Dutch-type cheeses. During cheese ripening, these bacteria encounter long periods of extreme nutrient limitation severely reducing the growth rate. However, they can survive these periods while still contributing to flavour formation. In this study, aroma formation by *L. lactis* and *Lc. mesenteroides* was studied at near-zero growth rates using retentostat cultivation. Moreover, both species were grown in retentostat co-cultures because this could potentially increase the aroma complexity by metabolic complementation (Erkuk et al., 2013) similar to found for co-cultivation of yeasts (van Rijswijk et al., 2017). Thereby, this study provides insights into the production of cheese aroma compounds outside the cheese matrix, which could be applied as food supplements in dairy or non-dairy products.

In retentostat mono-cultures, the physiological response of both species towards the near-zero growth rates was similar. During 35 days of retentostat cultivation, the biomass concentration increased 8 and 6-fold for *L. lactis* and *Lc. mesenteroides*, respectively, while the growth rates decreased to less than  $0.001 \text{ h}^{-1}$ . The viability remained above 80% throughout the cultivations. However, a large fraction of the *L. lactis* and *Lc. mesenteroides* cells lost the viability to grow on agar plates. Dynamic modelling of the biomass accumulation showed that the maintenance requirements of both *L. lactis* and *Lc. mesenteroides*

	<i>Lactococcus</i>	<i>Leuconostoc</i>	Co-culture
Ethanol	Black	Black	Black
Acetic acid	Black	Black	Black
Butanoic acid	Black	Black	Black
Hexanoic acid	Black	Black	Black
Nonanoic acid	Black	Black	Black
2-Butanone	Black	Black	Black
2-Heptanone	Black	Black	Black
1-Nonanol	Black	Black	Black
1-Dodecanol	Black	Black	Grey
2-Methyl-1-butanol	Black	Black	Black
3-Methyl-1-butanol	Black	Black	Black
3-Methyl-2-butenal	Black	Black	Black
3-Methyl-3-buten-1-ol	Black	Black	Black
3-Methyl-2-buten-1-ol	Black	Black	Black
Dimethyltrisulfide	Black	Black	Black
3-(Methylthio)propanal	Black	Black	Black
3-(Methylthio)-1-propanol	Black	Black	Black
Phenylethanol	Black	Black	Grey
Benzylalcohol	Black	Black	Black
Benzeneacetaldehyde	Black	Black	Black
Benzaldehyde	Black	Black	Black
Acetophenone	Black	Black	Black
Phenol	Black	Black	Black
2,5-Dimethylpyrazine	Black	Black	Black
1-(Methylphenyl)ethanol	Black	Black	Black
3-Hydroxy-2-butanone (Acetoin)	Black	White	Black
2,3-Butanedione (Diacetyl)	Black	Grey	Black
2,3-Pentanedione	Black	White	Grey
Tridecanal	Black	White	Black
Pentadecanal	Black	White	Black
Ethyl formate	Black	White	Black
Ethyl butanoate	Black	White	Black
Ethyl hexanoate	Black	White	Grey
Ethyl octanoate	Black	White	Black
Ethyl decanoate	Black	White	Black
Octanoic acid	Black	White	Black
1-Tetradecanol	Black	White	Grey
1-Hexadecanol	Black	White	Grey
3-Methyl-1-hexanol	Black	Grey	Black
2,6-Dimethylpyrazine	Black	White	Grey
Dimethylsulfone	Black	White	Black
Trimethyloxazole	Black	White	Grey
2-Ethyl-1-hexanol	White	Black	Black
1-Decanol	White	Black	Black
Ethyl acetate	White	Black	Grey
Ethyl lactate	White	Black	Black
2-Propanol	White	Black	Grey

**Fig. 7.** Presence (black) and absence (white) of the aroma compounds in retentostat mono- and co-cultures of *L. lactis* and *Lc. mesenteroides*. For mono-cultures, grey filling is used for compounds that were produced by both species, but with at least 8-fold difference in maximum abundance. For co-cultures, grey filling is used for compounds that were produced in co-cultures, but with at least an 8-fold lower maximum abundance compared to the mono-cultures.

decreased 7-fold at near-zero growth rates compared to chemostat cultures. Most likely this was caused by a reduction in protein turnover, which is one of the major constituents of the maintenance requirements (Kempes et al., 2017; van Mastrigt et al., 2018a). In contrast, previous studies revealed that the maintenance requirement of *L. lactis* KF147, isolated from the nutrient-poor plant environment, did not decrease at near zero-growth rates (Ercan et al., 2013). Both strains used in the current study were directly isolated from the nutrient-rich dairy environment and therefore they might have evolved a similar response but a different response compared to the plant-derived *L. lactis* KF147.

The dynamic models of the mono-cultures were used to predict the biomass accumulation of both species in a retentostat co-culture and this was verified in two independent co-cultures. The model predicted the biomass accumulation in the co-cultures surprisingly well, despite the simple assumptions of distribution of substrates (lactose and citrate) over the species based on their biomass concentration and no growth stimulation or inhibiting interactions. This showed that both species

competed mainly at the level of nutrient uptake and not by for instance bacteriocin-induced killing or mutualistic cross-feeding such as with yoghurt cultures (Settachaimongkon et al., 2014). It has been suggested that *Leuconostoc* promotes the growth of citrate-positive *Lactococcus* strains in fermented dairy products (Frantzen et al., 2017). However, no experimental support was given and such growth promotion could not be confirmed in this study.

*L. lactis* increased its abundance relative to *Lc. mesenteroides* right from start and a ratio of approximately 100:1 was obtained at the end of the co-cultivations. This ratio corresponds well with ratios found in cheese (Erkus et al., 2013; Frantzen et al., 2017). The dominance of *L. lactis* can be explained by i) its more efficient metabolism (homo-fermentative versus heterofermentative), ii) its higher maximum biomass yield on ATP and iii) its lower maintenance requirements.

To determine if co-cultivation could enhance the aroma complexity and to identify compounds that were specific for *L. lactis* and *Lc. mesenteroides*, aroma compounds were quantified in mono- and co-cultures

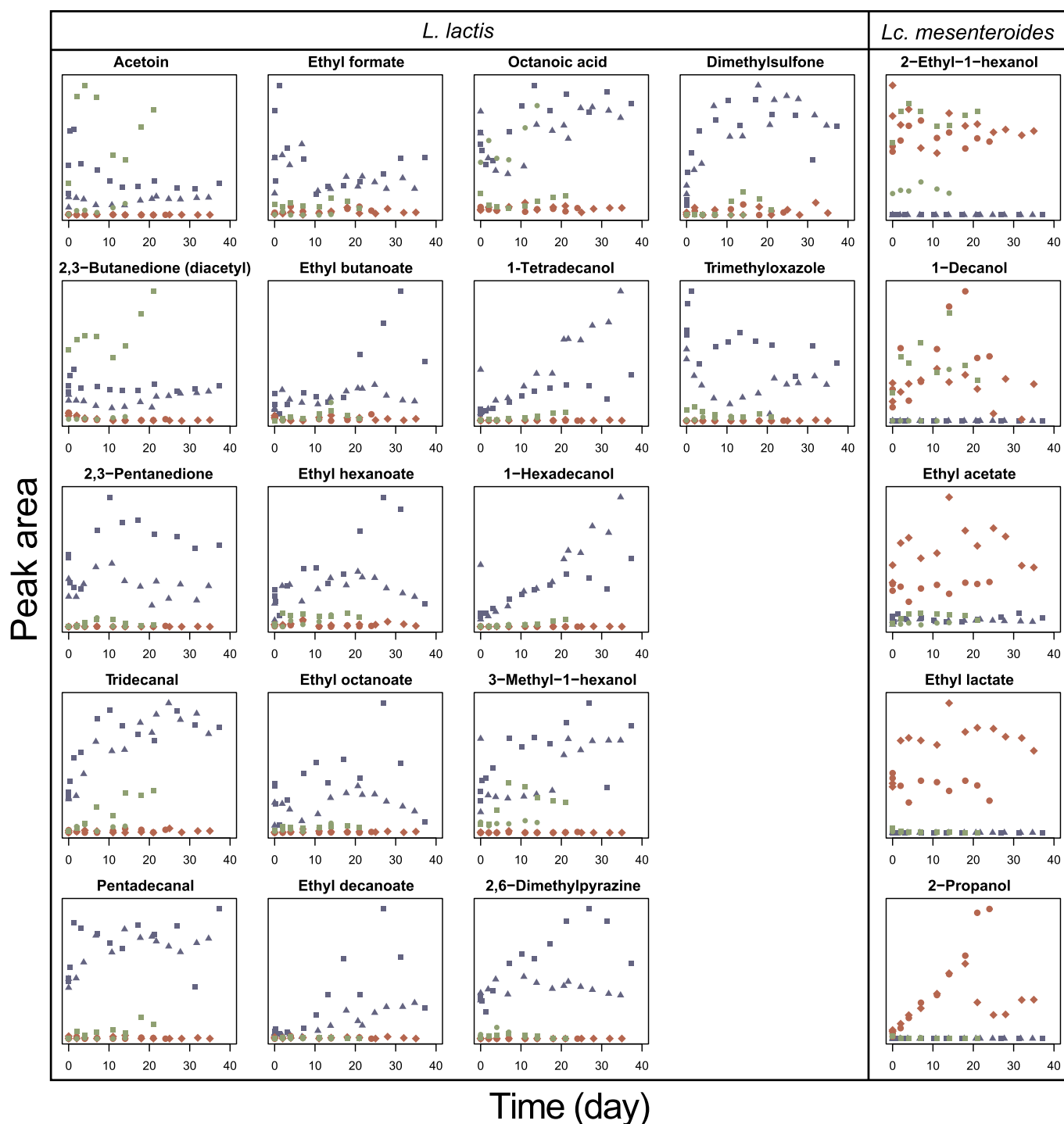


**Fig. 8.** Quantitative comparison of the abundance of species-specific aroma compounds in retentostat mono-cultures of *L. lactis* (blue) and *Lc. mesenteroides* (red) and in co-cultures (green). Symbols represent independent cultivations. Only compounds that were specifically produced by one of the species in the mono-cultures are shown. (For interpretation of the references to colour in this figure legend, the reader is referred to the Web version of this article.)

by HS SPME GC-MS. Compounds that were specific for *L. lactis* include mainly medium and long-chain fatty acids and their derived products (alcohols, aldehydes, methyl ketones and esters), acetoin and diacetyl. Since no fat or fatty acids were present in the medium, it can be concluded that the medium and long-chain fatty acids were synthesised by the bacteria. Compounds specific for *Lc. mesenteroides* include small esters (ethyl lactate and ethyl acetate), 2-propanol, and two primary alcohols (1-decanol and 2-ethyl-1-hexanol). Ethanol, lactate and acetate were also abundant in mono-cultures of *L. lactis* showing that the substrate specificities of the alcohol acyltransferases of *Lc. mesenteroides*

FM06 and *L. lactis* FM03-V1 differ, the former being more active on small acids. The specific production of 2-propanol by *Lc. mesenteroides* contrasts with the decreased amount in 2-propanol observed in cheese to which *Lc. mesenteroides* was added (Pedersen et al., 2016).

Co-cultivation could result in increased aroma complexity as found for co-cultivation of *Saccharomyces cerevisiae* and *Cyberlindnera fabianii* (van Rijswijk et al., 2017). In our study, specific *Lc. mesenteroides* aroma compounds were found in the co-cultures despite its low abundance (1%) showing that retentostat co-cultivation could increase the aroma complexity compared to mono-cultures as both bacteria were

retained. However, co-cultures lacked unique additional compounds. This might be caused by the large difference in abundance, which resulted in many *L. lactis* cells with few compounds specific for *Lc. mesenteroides* and vice versa.

For this situation where co-cultures lacked unique compounds, mixing mono-cultures might have an advantage over co-cultivation. Mixing mono-cultures would allow for better control of the ratio of the species-specific aroma compounds and therefore might be preferred when using these aroma compounds as food supplements in dairy or non-dairy products.

In conclusion, it is possible to grow *L. lactis* and *Lc. mesenteroides* in retentostat co-cultures and both bacteria were retained and stayed viable throughout the cultivations. However, the increase in the aroma complexity by co-cultivation was limited, possibly due to the dominance of *L. lactis*. The dynamic models described in this study excellently predicted the biomass concentrations in the co-cultures and could be a useful tool in selecting proper combinations of strains for retentostat co-cultivations, which could be used to produce aroma compounds that can be applied as food supplements.

### Acknowledgements

This work was supported by Arla Foods (Aarhus, Denmark).

### Appendix A. Supplementary data

Supplementary data to this article can be found online at <https://doi.org/10.1016/j.fm.2019.01.016>.

### References

- Boender, L.G.M., de Hulster, E.A.F., van Maris, A.J.A., Daran-Lapujade, P.A.S., Pronk, J.T., 2009. Quantitative physiology of *Saccharomyces cerevisiae* at near-zero specific growth rates. *Appl. Environ. Microbiol.* 75, 5607–5614. <https://doi.org/10.1128/Aem.00429-09>.
- Cogan, T.M., Jordan, K.N., 1994. Metabolism of *Leuconostoc* bacteria. *J. Dairy Sci.* 77, 2704–2717. [https://doi.org/10.3168/jds.S0022-0302\(94\)77213-1](https://doi.org/10.3168/jds.S0022-0302(94)77213-1).
- Ercan, O., Smid, E.J., Kleerebezem, M., 2013. Quantitative physiology of *Lactococcus lactis* at extreme low-growth rates. *Environ. Microbiol.* 15, 2319–2332. <https://doi.org/10.1111/1462-2920.12104>.
- Erkus, O., de Jager, V.C.L., Geene, R.T.C.M., van Alen-Boerrigter, I., Hazelwood, L., van Hijum, S.A.F.T., Kleerebezem, M., Smid, E.J., 2016. Use of propidium monoazide for selective profiling of viable microbial cells during Gouda cheese ripening. *Int. J. Food Microbiol.* 228, 1–9. <https://doi.org/10.1016/j.ijfoodmicro.2016.03.027>.
- Erkus, O., de Jager, V.C.L., Spus, M., van Alen-Boerrigter, I.J., van Rijswijck, I.M.H., Hazelwood, L., Janssen, P.W.M., van Hijum, S.A.F.T., Kleerebezem, M., Smid, E.J., 2013. Multifactorial diversity sustains microbial community stability. *ISME J.* 7, 2126–2136. <https://doi.org/10.1038/ismej.2013.108>.
- Frantzen, C.A., Kot, W., Pedersen, T.B., Ardö, Y.M., Broadbent, J.R., Neve, H., Hansen, L.H., Dal Bello, F., Østlie, H.M., Kleppen, H.P., Vogensen, F.K., Holo, H., 2017. Genomic characterization of dairy associated *Leuconostoc* species and diversity of *Leuconostoc* in undefined mixed mesophilic starter cultures. *Front. Microbiol.* 8, 132. <https://doi.org/10.3389/fmicb.2017.00132>.
- Hughenoltz, J., 1993. Citrate metabolism in lactic acid bacteria. *FEMS Microbiol. Rev.* 12, 165–178. [https://doi.org/10.1016/0168-6445\(93\)90062-e](https://doi.org/10.1016/0168-6445(93)90062-e).
- Kempes, C.P., van Bodegom, P.M., Wolpert, D., Libby, E., Amend, J., Hoehler, T., 2017. Drivers of bacterial maintenance and minimal energy requirements. *Front. Microbiol.* 8, 31. <https://doi.org/10.3389/fmicb.2017.00031>.
- Pedersen, T.B., Vogensen, F.K., Ardö, Y., 2016. Effect of heterofermentative lactic acid bacteria of DL-starters in initial ripening of semi-hard cheese. *Int. Dairy J.* 57, 72–79. <https://doi.org/10.1016/j.idairyj.2016.02.041>.
- Schmitt, P., Diviès, C., Merlot, C., 1990. Utilization of citrate by *Leuconostoc mesenteroides* subsp. *cremoris* in continuous culture. *Biotechnol. Lett.* 12, 127–130. <https://doi.org/10.1007/bf01022428>.
- Settachaimongkon, S., Nout, M.J.R., Antunes Fernandes, E.C., Hettinga, K.A., Vervoort, J.M., van Hooijdonk, T.C.M., Zwietering, M.H., Smid, E.J., van Valenberg, H.J.F., 2014. Influence of different proteolytic strains of *Streptococcus thermophilus* in co-culture with *Lactobacillus delbrueckii* subsp. *bulgaricus* on the metabolite profile of set-yoghurt. *Int. J. Food Microbiol.* 177, 29–36. <https://doi.org/10.1016/j.ijfoodmicro.2014.02.008>.
- van Mastrigt, O., Abee, T., Lillevang, S.K., Smid, E.J., 2018a. Quantitative physiology and aroma formation of a dairy *Lactococcus lactis* at near-zero growth rates. *Food Microbiol.* 73, 216–226. <https://doi.org/10.1016/j.fm.2018.01.027>.
- van Mastrigt, O., Abee, T., Smid, E.J., 2017. Complete genome sequences of *Lactococcus lactis* subsp. *lactis* bv. diacetylactis FM03 and *Leuconostoc mesenteroides* FM06 isolated from cheese. *Genome Announc.* 5 e00633-17. <https://doi.org/10.1128/genomeA.00633-17>.
- van Mastrigt, O., Gallegos Tejeda, D., Kristensen, M.N., Abee, T., Smid, E.J., 2018b. Aroma formation during cheese ripening best resembled by slow-growing in retentostat cultures. *Microb. Cell Factories* 17, 104. <https://doi.org/10.1186/s12934-018-0950-7>.
- van Mastrigt, O., Mager, E.E., Jamin, C., Abee, T., Smid, E.J., 2018c. Citrate, low pH and amino acid limitation induce citrate utilisation in *Lactococcus lactis* biovar diacetylactis. *Microb. Biotechnol.* 11, 369–380. <https://doi.org/10.1111/1751-7915.13031>.
- van Rijswijck, I.M.H., Wolkers – Rooijackers, J.C.M., Abee, T., Smid, E.J., 2017. Performance of non-conventional yeasts in co-culture with brewers' yeast for steering ethanol and aroma production. *Microb. Biotechnol.* 10, 1591–1602. <https://doi.org/10.1111/1751-7915.12717>.
- Yvon, M., Rijnen, L., 2001. Cheese flavour formation by amino acid catabolism. *Int. Dairy J.* 11, 185–201. [https://doi.org/10.1016/S0958-6946\(01\)00049-8](https://doi.org/10.1016/S0958-6946(01)00049-8).